Hindawi
Journal of Sensors
Volume 2022, Article ID 7419031, 15 pages
https://doi.org/10.1155/2022/7419031

Research Article

Modeling Land Use Change in Sana'a City of Yemen with MOLUSCE

Eman A. Alshari[1,2] **and Bharti W. Gawali**[2]

[1]*Thamar University, Computer Science & Information Technology, Dhamar, Yemen*
[2]*Dr. Babasaheb Ambedkar Marathwada University, Aurangabad 431004, India*

Correspondence should be addressed to Eman A. Alshari; em.alshari3@gmail.com

Received 23 June 2022; Revised 29 August 2022; Accepted 17 September 2022; Published 20 October 2022

Academic Editor: Rajesh Kaluri

This study provided insight into the size of the difference between the actual and predicted changes in Landsat 8 satellite imagery for the case study Sana'a of Yemen. The LULC classification was created using data available in 2005, 2010, 2015, and 2020. It used the MOLUSCE tool for predicting land changes for the predicted for 2010, 2015, 2020, 2025, and 2030. The objectives of this study are 1) To compare the actual and predicted land changes in 2010,2015 and 2020. 2) To analyze and verify the tool's performance (MOLUSCE). 3) To identify the size of effect which evented land changes in 2015 on land changes in 2020,2025 and 2030. The results were: 1/the effects of land changes in 2010 showed the accuracy and reliability of MOLUSCE for predicting land changes due to the low difference between the actual and predicted 2010 before the conflict in the region. 2/the actual changes for 2015 were negative and did not support the logical trend toward progress where it is natural that the human element progresses to the increasing construction. 3/identify prediction changes for (2020,2025,2030) are affected by events conflict, which showed in the results of the 2015 images.

1. Introduction

For a planning strategy for managing land use and land cover, it is necessary to identify the prediction of future land changes [1]. There are many benefits, and it is often used as an indicator of human impact on land change processes for various adequacy measures [2]. Multiple theories can predict the future state of a system based only on the form that preceded it [3]. Creating a transitional probability matrix for LULC change from period 1 to two allows for predicting future change [4]. The researcher used multispectral satellite imagery and the MOLUSCE model to predict LULC change in different regions. It also calculates the transfer rates between other land uses and estimates their conditions [5, 6].

MOLUSCE is Modules of Land Use Change Evaluation. It is a computer application for analyzing, modeling, and simulating changes in LULC [7, 8]. The plugin has well-known algorithms for land use/cover change analysis, urban analysis, and forestry projects and applications [8]. Regarding geographical analysis, Modeling, and changing transition potentials, techniques for understanding LULC mechanisms have advanced quickly [9]. Effective and repeatable simulation models can be used to explore the factors influencing past, present, and future projections and their significance in various situations [10]. Regionally distributed models for analysing and projecting LULC include Dinamica [11], Markov-FLUS [12], SLEUTH cellular automata [13], artificial neural network-Markov chain [14], CA-ANN [15], and CLUE-S [16]. The LULC concerns are addressed differently in each model [17]. Because they successfully reflect nonlinear spatially probabilistic land-use shifts, neural network models are often employed to simulate LULC [18]. When combined with other methodologies, CA can be a valuable tool for understanding land-use systems and their underlying dynamics [19].

Work of the MOLUSCE: Modeling and simulation tasks are made more straightforward for users with MOLUSCE's user-friendly and intuitive plugin. Seven primary elements

make up the graphical user interface (GUI) explain the MOLUSCE plugin: Inputs, Evaluation Correlation, Area Changes, Transition Potential Modeling, Cellular Automata Simulation, Validation, and Messages are listed in that order [20].

This study is distinct and unique compared to other literature studied in the same field example, Muhammad et al. [4] conducted a study aimed: at the evolution of spatio-temporal LULC trends over the preceding four decades. The predicting LULC in the future utilizes socioeconomic and environmental factors. The determining LULC change's size and potential impacts on the regional pattern. Choosing the LULC intensity situation in the future while this research focuses on the following goals: 1) To compare the actual and predicted land changes in 2010,2015, and 2020. 2) To analyze and verify the tool's performance (MOLUSCE). 3) To identify the size of effect which evented land changes in 2015 on land changes in 2020,2025 and 2030.

The comparison helps determine the scope of the possibility and accuracy of the tool used to forecast land changes in the event that the situation in the researched area is steady. The comparison between the actual and predicted changes in the land has a substantial and influential role in measuring the extent of the land changes that occurred in the region and the extent of the impact of the events on Land changes in the event that the region was subjected to sudden and unexpected events like the conflict with missiles and an attack on the destruction of the land, such as what happened to the area of this current study. The two situations were combined in the current research, making it noteworthy and valuable for professionals and those who are curious about the topic.

The significance of the current study is to identify the difference between actual change and predictive change in to study area to estimate the changes in land, to know the extent the size of those losses to try to develop those countries during the passage of that period, and this formed the strong motivation for researchers.

The results have been done through Modeling and simulating land use spatial patterns. Traditional land-use planning assumes that infrastructure will not change. Further facility improvements can be required if a zone's population or activity grows. In this study, the (DEM, slope, aspect, distance from the road, and distance from built-up) are used as learning processes for spatial variable maps to evaluate their effects on LULC.

The findings showed that: 1. size of the difference between actual and predicted changes for land changes in 2015 affected by events conflict. The actual changes for 2015 were negative and unfavorable and did not follow the logical trend of advancement. 2/Prediction for (2010 and 2020) lend credence to the logical upward trend in advancement and the endeavor to follow a reasonable, incremental trend toward improving prediction changes for 2025–2030. 4/The discrepancy between the actual and projected land changes for 2010, before the war in the region, was so small, so the results demonstrated the accuracy and dependability of MOLUSCE for launching land changes.

This study also clarifies the primary forms of the surface and areas of human influence on it, how to exploit various future development areas, and identifies risk places in the study area. A comparison of findings of the study revealed that the 2015 map was a dividing line in the changes that occurred in Sana'a, which showed that before 2015, the capital was in better shape. Sana'a was progressing in urban area density, with an increased built-up area. After 2010 the built-up area decreased. The results of this research will assist in monitoring and predicting future land use and cover changes. Policymakers and decision-makers can use the study's findings to address the exploitation of natural resources in dry areas.

The contribution of this research is the evaluation of the MOLUSCE plugin's precision and dependability. Creation of analytical comparison for identifying the difference between actual and predicted land changes for LULC in Sana'a city of Yemen in (2010,2015, and 2020) of Landsat8 satellite. Identify prediction changes for (2020,2025,2030) are affected by events conflict, which showed in the results of the 2015 images.

2. Related Works

2.1. Review of Existing Works. Multiple challenges associated with past, present, and future land-use patterns, weather patterns, soil dynamics, carbon, and climate change are intertwined with land transformation. Utilizing particular software or techniques to estimate or compute those disparities is challenging. A substantial drive and inspiration for this research came from reviewing earlier studies. The rate of change can be clarified, essential components of LULC change can be highlighted, and alternative LULC scenarios can be created to predict future land use demand [21].

This section will discuss the most important and recent studies in the same field with the tool (MOLUSCE) used in prediction for identifying land changes predicated. Previous research [22–31] has shown that dealing with the MOLUSCE plugin is recent. The beginning of its Appearance after 2010. And predicting future land changes requires taking into account the past, present, and future scenarios [31–36]. Predictions of land changes have been made long, commencing in early 1930 [37]. It was the initial SLEUTH model, which the researchers employed for a long time before moving on to CA-Markov in 1980 [38]. It was used to predict land changes after 2010 [39]. According to the survey, the researchers focused solely on the analysis of land change predictions, not on comparing actual and predicted land changes, indicating a gap that led to the creation of this study [40–51].

Kamaraj and other authors have researched using the MOLUSCE plugin (MLP-ANN) model in the QGIS 2.18.24 version of forecasting. They established potential land-use changes in the years 2025 and 2030 to detect the transition of land-use changes in the Bhavani basin for 2005 and 2015 [20].

To forecast future changes in LULC and LST, Zhang and colleagues used cellular automata (CA) and artificial neural networks (ANN). Their findings demonstrated the growth of Wuhan's built-up area [52].

The work by Rahaman and colleagues presented here evaluated the capacity of the SVM and CA algorithms to

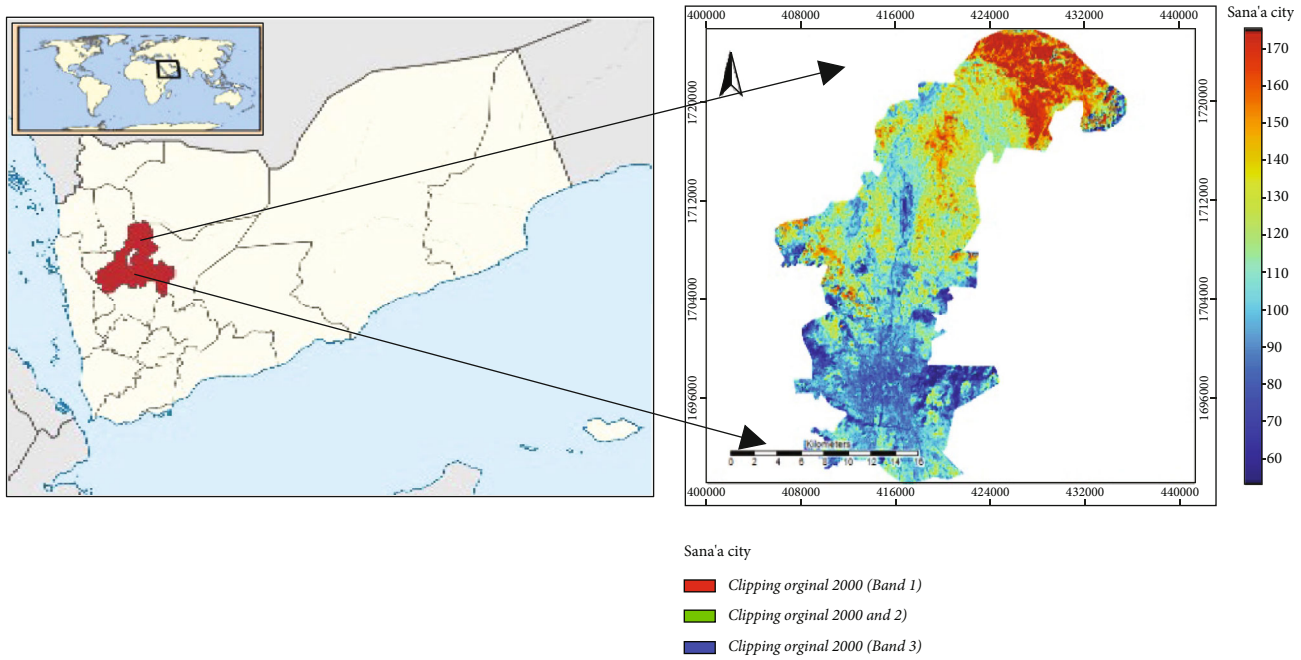

Figure 1: Location of the case study.

track (2005–2020) and forecast (2025 and 2035) the future LULC change in Penang, Malaysia. The LULC classes were estimated using Landsat photos, and the CA model was validated using Pearson chi-square values [53].

Explored by Kafy and others, the relationship between LULC indexes (NDVI, NDBI, NDBaI, and NDWI) and LST, as well as the distribution of LST across various land use categories, is how LULC change affects land surface temperature (LST). The LULC and LST maps for the years 2029 and 2039 were simulated using the Multi-Layer Perceptron-Markov Chain (MLP-MC) and Artificial Neural Network (ANN) methods, respectively [54].

2.2. The Study Area. Sana'a is the case study for this article [34], as it is one of Yemen's largest cities and the capital of the same-named province. Sana'a is located at 15°N 44°C, or 15.369445 latitudes 44.1191006, with GPS coordinates of 15°22' 10.0020'N and 44°11' 27.6216'E [35]. Sana'a has a total size of 126 km2 (49 sq mi) and a population of 2,545,000 as of 2017 [36]. The city is approximately 2,200 meters above sea level [38], as appears in Figure 1. With a complete space of 126 km2 (49 sq mi), it has a populace of around 3,937,500 (2012) [39]. Sana'a's precipitation is limited to 200 mm/year, while the fading is several times higher. The average daily sunlight-based irradiance ranges from 800 to 1400 mol/m^2, with an average air temperature between 22-30°C at low humidity levels (35-55%). Its climatic conditions (temperature, sun-based radiation) are ideal for wastewater treatment based on phototrophic [40].

Figures 2 and 3 images indicate land changes in Sana'a recently. After 2015, that change has a role in analyzing this study. This study showed the differences in geomorphology during the mentioned period through the land change classification, which suggests that land use in this re∗gion is inappropriate. A database of LULC of Sana'a was created in this work.

Such research is necessary for developing nations because it will aid in managing natural resources, where LUCC plays a critical role in regional economic development and natural resource management. Destroyed the country's infrastructure, preventing Sana'a's vital economic, social, environmental, health, and agricultural development.

2.3. Collecting Data of Satellite. The Landsat8 Satellite Sensor (30 m) and the mathematically open-source Landsat8 MSS/TM were utilized in this work for LULC mapping. The image was taken by the United States Geological Survey (USGS) in the Sana'a region, a scientific body of the US government. The base map [30] was created from survey pictures of the SOI toposheet at sizes of 1 : 50000. The data was collected in the time intervals of 2005, 2010, 2015, and 2020, and the database details are provided in Table 1. Figure 4 shows a data set from the Landsat8 Satellite Sensor (30 m) capture and selection region analysis using Composite band 432.

Note: Operational Land Imager (OLI) and Thermal Infrared Sensor (TIRS), Thematic Mapper (TM) Enhanced Thematic Mapper Plus (ETM+) and Multispectral Scanner (MSS).

3. Research Methodology

Work of the MOLUSCE: Modeling and simulation tasks are made more straightforward for users with MOLUSCE's user-friendly and intuitive plugin. This study includes seven basic steps for Modeling using MOLUSCE. Seven primary steps make up the graphical user interface (GUI) explain the MOLUSCE plugin: Inputs, Evaluation Correlation, Area

Figure 2: Buildings & Infrastructure of Sana'a city before the conflict [3].

Figure 3: Images & Land Changes for Sana'a City After Conflict [37].

Table 1: Images collected & used in this study of Sana'a city.

No	Date acquired	Satellite	Sensor	Spatial resolution
1	2005	Landsat 7	Enhanced thematic mapper plus (ETM+)	30 m
2	2010	Landsat 8	Thematic mapper (TM)	
3	2015	Landsat 8	Operational land imager (OLI) & thermal Infrared sensor (TIRS)	
4	2020	Landsat 8	Operational land imager (OLI) & thermal Infrared sensor (TIRS)	

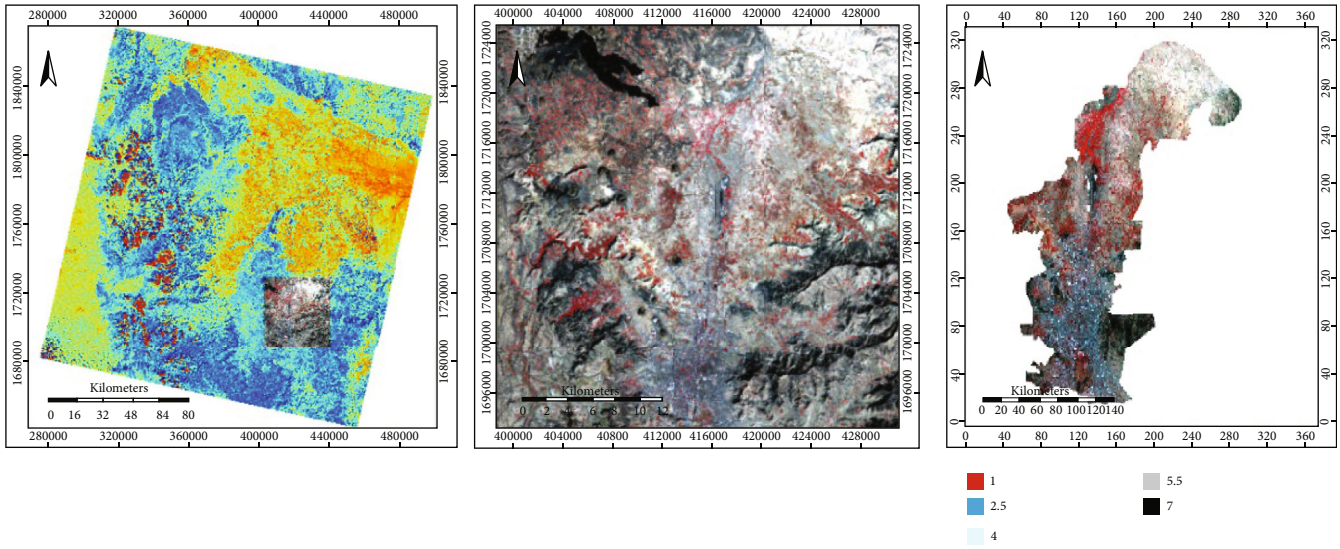

Figure 4: Data set of Landsat8 Satellite Sensor with clipping of study area (false color composite, bands 432).

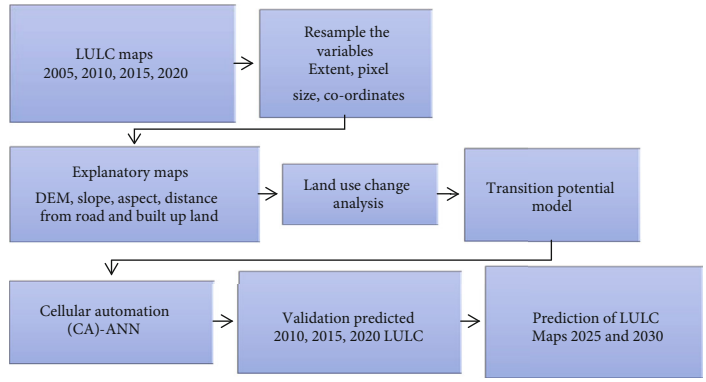

Figure 5: Methodology of this study.

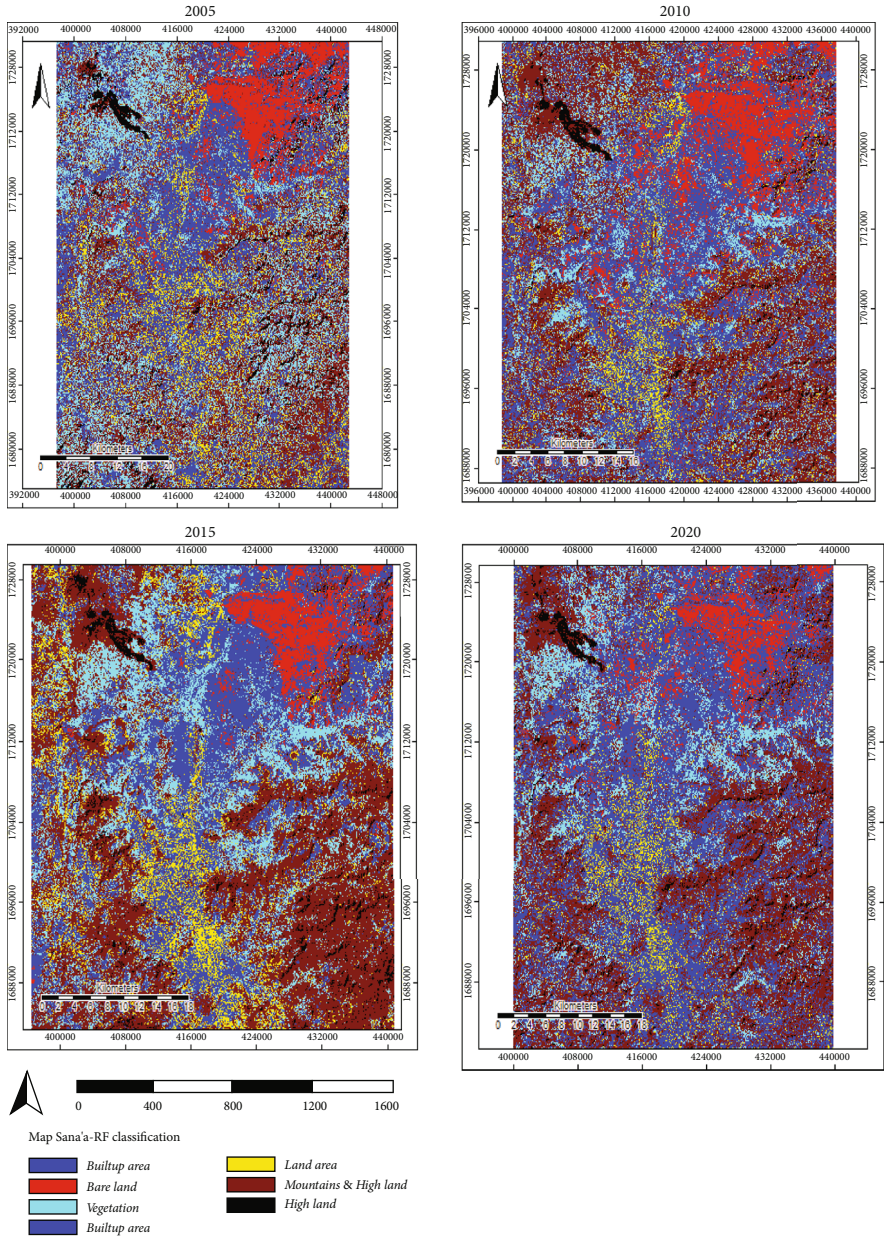

Figure 6: Classified Map for Sana'a over the five decades (2005–2020).

Table 2: Description of LULC classes in the study area.

LCLU class	Description
High land	High land remote may be settlements and clans with a long history and profound loyalties.
Mountains	A mountain is a raised section of the earth's crust with steep sides and exposed bedrock.
Land area	The area in square kilometers of the land-based portions of conventional geographic regions is referred to as land area, which population peoples. Not contains buildings, maybe streets, parks, roads or buildings crashed down, like this.
Builtup	Builtup areas may be large buildings, small buildings, settlements, transportation, land, or places containing people like banks, schools, hospitals, etc.
Vegetation	Space containing crops, fields, sparse grassland, a temperate steppe, and a temperate meadow.
Bare land	Bare soil, bare rocks, and land do not contain people like the desert.

Table 3: Analysis of Land changes for years 2010,2015,2020.

No	Class	Actual 2005		Actual 2010		Actual 2015		Actual 2020	
		Area km^2	%	AREA km^2	%	AREA km^2	%	AREA km^2	%
1	High land	1716120	0.84%	316881	1.83%	492039	2.41%	892039	3.30%
2	Mountains	5788260	28.34%	5127039	29.61%	7512750	36.75%	3512750	12.99%
3	Land area	5096592	24.95%	957069	5.53%	1740402	8.51%	1340402	4.96%
4	Builtup area	24867360	12.17%	6952491	40.15%	6325785	30.94%	13325785	49.28%
5	Vegetation	5334408	26.11%	2224908	12.85%	3333969	16.31%	7333969	27.12%
6	Bare land	1549656	7.59%	1735965	10.03%	1037925	5.08%	6379250	2.36%
7	Total of area=	20427264	100%	316881	100%	492039	100%	8920390	100%

Table 4: Accuracy assessment of 2010,2015, and2020 classified images.

Class	2005		2010		2015		2020	
	Producer's accuracy	User's accuracy	Producer's accuracy	User's accuracy	Producer's accuracy	User's accuracy	Producer's accuracy	User's accuracy
High land	0	0	78	98.7179	77	100	77	100
Mountains	0	7.1559	0	0	0	0	0	0
Land area	109	95	0	0	96	100	96	100
Builtup area	20	100	1	100	58	100	58	100
Vegetation	371	0	371	100	371	100	371	100
Bare land	100	0	100	0	100	0	100	0
Kappa coefficients	0.99705	0	0.99425	0	1.0	0	1.0	0
Overall accuracy(%)	99.8%		99.6%		100%		100%	

Changes, Transition Potential Modeling, Cellular Automata Simulation, Validation, and Messages are listed in that order [20], but the steps prediction of land changes for the current study was as follows in Figure 5:

3.1. Actual Changes (LULC Maps 2005,2010,2015,2020). This study shows analysis classification for Sana'a city land from 2005 to 2020. LULC Classification was done in 2005, 2010, 2015, and 2020 using Random Forest of supervised machine learning algorithm within software SAGA. It can find LULC classified for Sana'a city, and the categories can be apparent in the differences in land change in Sana'a city, as shown in Figure 6. The software also generates the transition matrix, which shows the percentage of pixels switching from one kind to the next. As input layers for model processing, there are six samples for six parameters for creating model classes: High Land, Mountains, Land Area, Built-up, Vegetation, and Bare Land. Note to parameters in software SAGA with these models classification in down are seven, but in processing and results in the parameter are six since merge area vegetation with agriculture land. Create the samples depending on RGB color composites of sentinel-2A images, for example, the class Vegetation (red pixels in color composite RGB =432), detailed changes in the region. The following illustrates the critical description of class input in Table 2.

It was implying that the poor state of Sana'a city was caused by the war, with increasing built-up area in town resulting in a decrease in land area and the decreasing

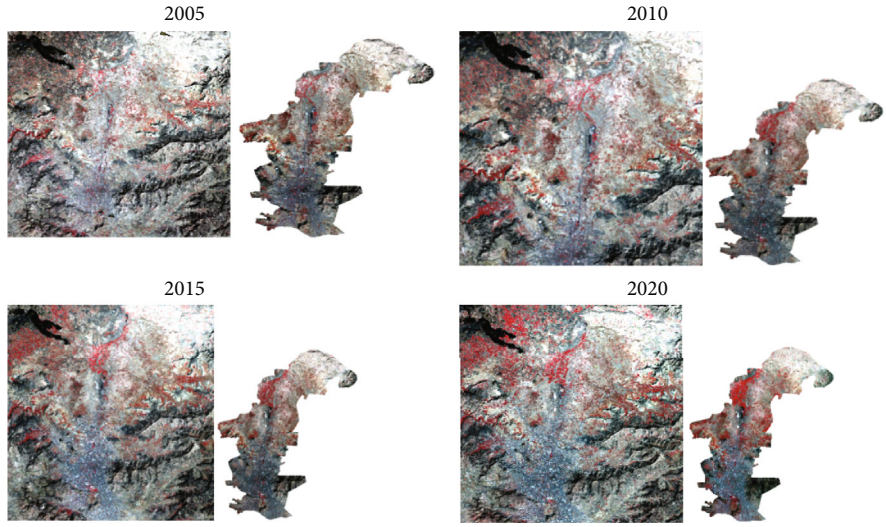

Figure 7: Pre-processing satellite images for classification.

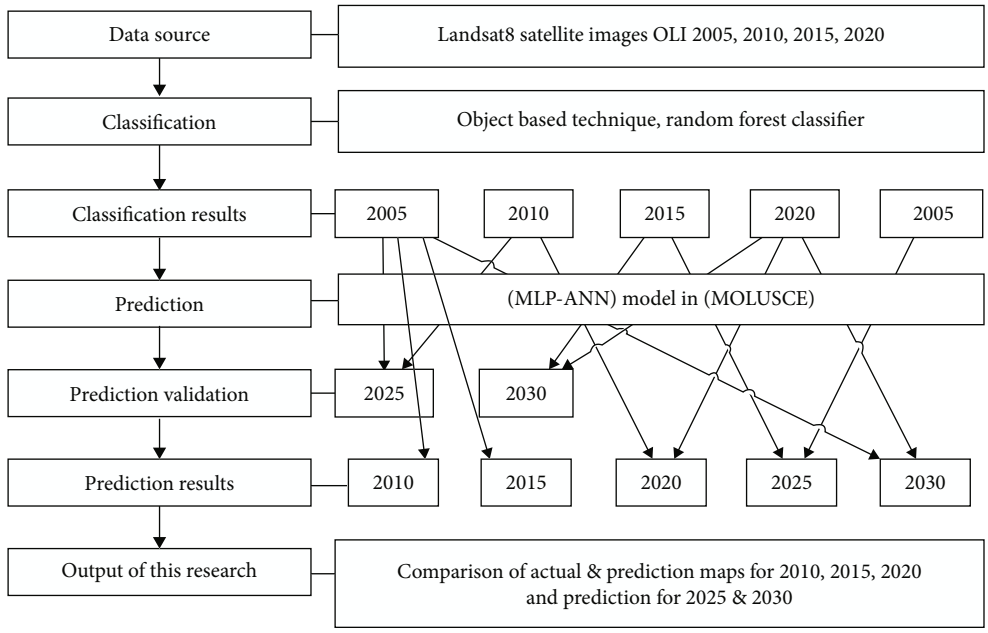

Figure 8: Details Steps process of Predicting land use change in this study.

built-up area in the city's growing land area. The findings revealed that the political problem began after 2010, as the built-up area decreased on a map in 2010 while the land area increased. Increasing built-up area in town results in a decrease in land area and the decreasing built-up area in the city growing land area. The LULC changes from 2005 to 2020 are summarized in Table 3, showing the spatial variation from 2005 to 2020. The region's area in 2005 was 20427264 km^2 , and in 2020 was 892039 km^2. In 2005, the built-up area was 12.17%, bare land was 7.59%, vegetation was 26.11%, high ground was 0.84%, the land area was 24.95%, and mountains were 28.34%. In 2020, the built-up area was 49.28%, bare land was 2.36%, vegetation was 27.12%, high ground with 3.30%, the land area was 4.96%, and mountains were 12.99%. Trend changes were seen for all LULC categories during 2005, 2010, 2015, and 2020, except water bodies and grasslands.

Validation for actual changes is apparent in Table 4 illustrates the LULC categories' change probability matrix from 2005 to 2020. The value runs from 0 to 1, with greater values indicating more significant changes, except for the nation cells with higher values, which show no changes because they remain in the same category—the LULC analysis for every year, illustrating the trajectory of LULC change from 2005 to 2020. The precision of the producer, which is often used to compute the size of the region to be categorized, is the chance of successfully classifying pixels.

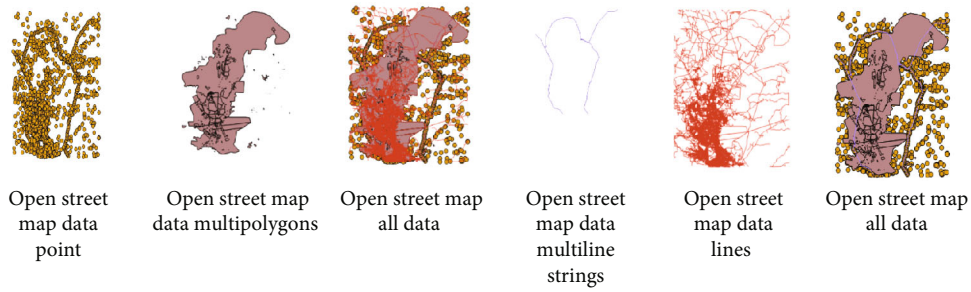

Figure 9: Details of Open Street Map Data.

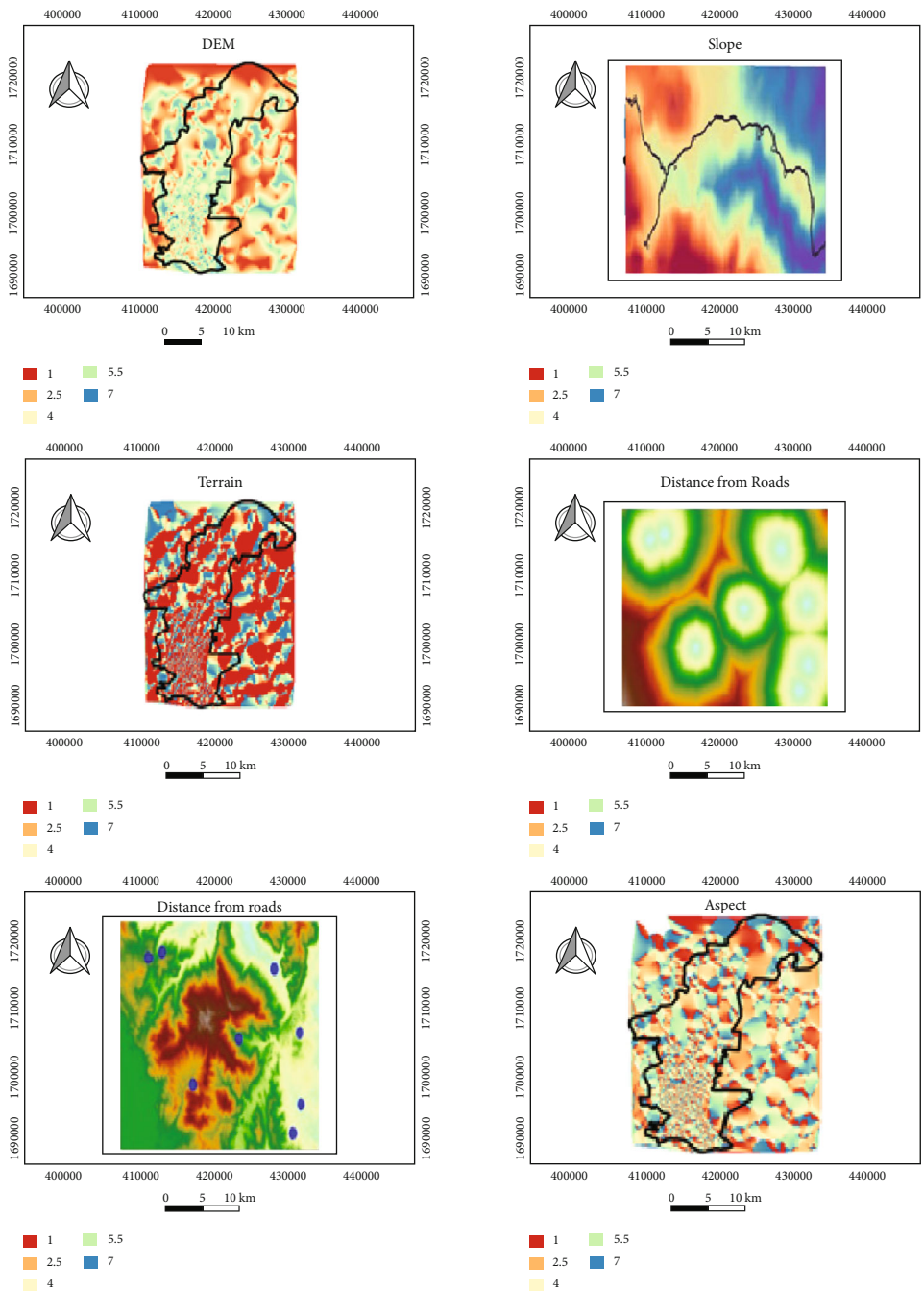

Figure 10: The criteria for process simulation land changes.

3.2. Predicting Land Use Change

3.2.1. Inputs. The model's first phase incorporates the LULC maps for the starting year (2005,20102015 and 2020) for predicate 2025 and 2030. The spatial variable components are given into the model to produce a land cover change map, from which the changing pattern for the study area between 2005 and 2020 is generated. These factors include the DEM, slope map, aspect map, distance from roads and rivers, and built-up density Figure 7.

The transition probabilities from the MLP-ANN learning process are employed in the study to describe the LULC changes. The following diagram illustrates the essential steps of this research study in Figure 8.

For the Prediction of LULC, the data is not overtly distributed, but its implementation is terminated by organizations responsible for managing satellites. Figure 9 will display the pre-processing corrections for Landsat 8 satellite images. That images cleared differences in these images map before classification. According to the colors of the Landsat satellite, the region's red color is vegetation, and the white color is bare land, light grey is land area & network road, and dark grey is a built-up area. Initially, the comparison is clear how to land Sana'a city is changed. Data set of Landsat8 Satellite Sensor (30 m) & selection area study with Composite band 432. Open Street Map Data is essential for preprocessing the simulation.

In MLP-ANN learning processes, the criteria for process simulation land changes in the future, such as DEM, slope, aspect, range from roads, and range from constructed, are used as spatial variable maps to estimate their effects on LULC 2010,2015 and 2020. The impacts were discovered to be significant. The model is down used to forecast LULC changes in 2010,2015, and 2020. The input module contains LULC maps from several epochs and biophysical and socioeconomic driving force data such as road networks, rivers, terrain, population, etc. Transition matrices for land change and land change maps are created. Simulation Maps of transition potentials are displayed, and a certainty function (experimental) and simulation result pre-processing for implementing the MOLUSCE model prediction is shown in Figure 10.

In this study, as input for the process, the simulation needs to prepare the maps applied in symbology selected from the list render type (single band pseudocolor), resulting in maps of this process and pre-processing maps for the prediction of symbology as shown in Figure 11.

3.2.2. Evaluation Correlation. Using Pearson's correlation, Crammer's coefficient, and Joint information uncertainty, the correlation of geographic variables between the two raster images—which are used to study the correlation among the geographical variables factors—is assessed. [52] The category of each region and the LULC changes are computed between the initial year (2010) and the end year (2030).

3.2.3. Area Changes. The experiment of the prediction process applied for the years 2015,2020,2025 & 2030 using the MOLUSCE to predict the land changes for classified maps. Figure 12 depicts the percentage shift from 0 to 100 per-

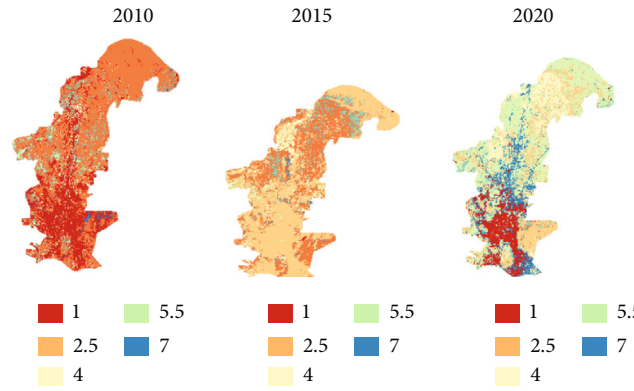

Figure 11: Pre-processing maps for prediction.

cent through time and between years. During the study period, changes in 2010 rose overall. Between 2010 and 2015, most of the land was degraded, and the arid lands grew. In the city center, there were several changes. Several studies have found that shifts in rapid population growth and economic development in the studied area are widespread since the globe is changing. The projection for 2015 was for an increase in structures and development, but the actual photographs revealed the opposite, with construction lands declining due to the region's deteriorating conditions. Over the city, changes in wet and arid terrain may also be seen.

We separated the study period into two brief periods, before 2015 and after 2015, and estimated the area of LCLU categories for the two periods to comprehend observational changes in the LCLU better. Meadows appeared initially in the lost space during the first phase, followed by forests in the northern sections. In terms of shrinking acreage, wetlands came in third.LCLU changes have been rapid in recent years, owing to population growth and rapid economic growth, both of which have had negative consequences for the environment and natural resources. The LCLU changed differently than it did in the first phase. The output of the prediction model between 2010,2015 decreased but increased between 2025 and 2030. The LULC maps of 2025 and 2030 were forecasted using the same spatial variable factor combinations of the LULC maps of 2005 and 2010.

3.2.4. Modeling of Transition Potential. The plugin uses artificial neural networks (ANN), weights of evidence (WoE), logistic regression (LR), and multi-criteria evaluation, among other techniques for constructing potential transition maps (MCE). Each methodology uses geographic information and land use/cover change data to calibrate and model land use/cover changes. This study employed the Artificial Neural Network (Multilayer Perception) technique to model LULC forecast and predict the LULC map for 2015. The kappa coefficient was determined when validating the actual and predicted LULC maps [52].

3.2.5. ANN-CA. A potential transitional map can be made in various ways, but this module also includes computational intelligence elements like artificial neural networks (ANN).

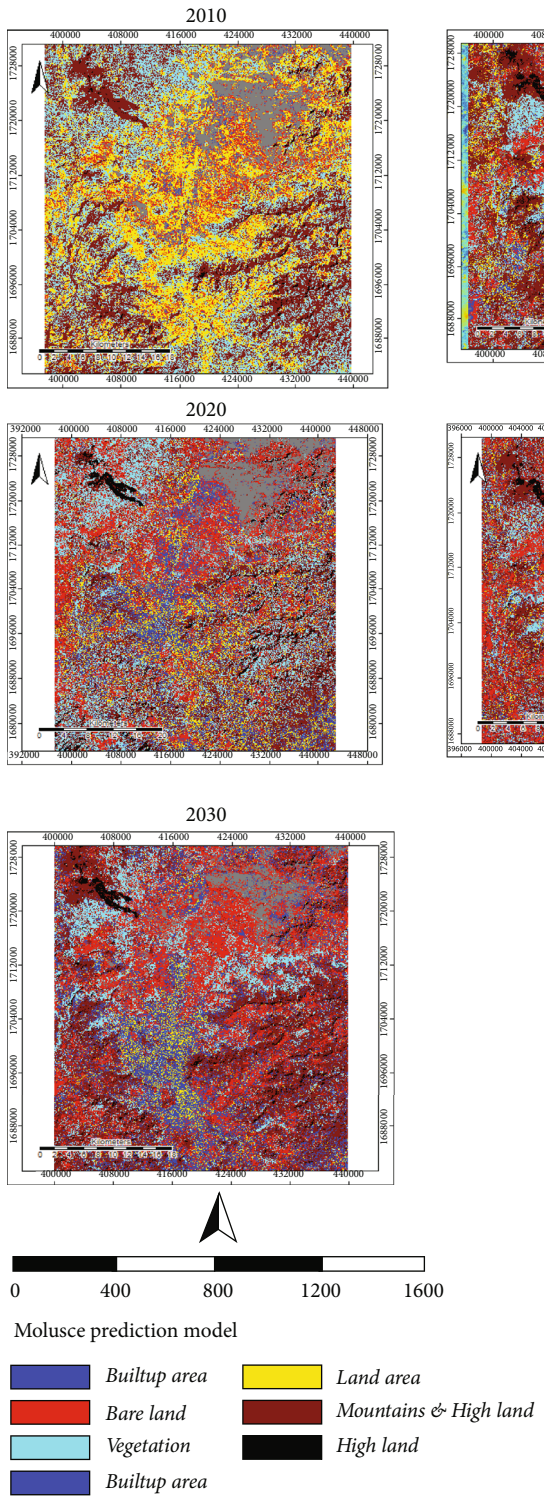

Figure 12: Predictions for 2010,2015,2020,2025, and 2030.

All techniques for calibrating and modeling LULC change use LULC data as input. This approach is appropriate for solving issues where the algorithm must handle massive amounts of ambiguous or challenging-to-implement input data. As a result, a continuous index is generated that rates the terrain from 0 to 1 and describes it. Due to fuzzy logic needs ANN, a continuous range, such as 0 and 1, is chosen based on usability. The crucial components of ANN are the interactions between connected neurons and the modification of the weight connections between them (Bhattacharya et al., 2020). When predicting the LULC map for the year 2015, the following parameters were finally determined: neighbourhood = 1, iterations = 1000, hidden layer = 10, momentum = 0, learning rate = 0.001 [52].

Table 5: Validation for Prediction Processes.

Variable in position	Kappa correctness percentage	Coefficients of kappa
DEM, range from the road, range from builtup	79.27%	0.72
DEM ranges from road	76.33%	0.63
DEM range from builtup	73.45%	0.61
DEM range from builtup, slope	74.01%	0.59
DEM, slope,aspect	71.86%	0.57

3.2.6. Validation. The kappa coefficient was commonly used to gauge how well LULC was evaluated. The comparison between the actual and predicted LULC maps is validated by determining the overall kappa value. The following expression is used to determine the Kappa coefficient [52].

$$\text{kappa} = \frac{(\text{po} - \text{pe})}{1 - \text{pe}} \quad (1)$$

Where po stands for the percentage of actual agreements, and pe for the percentage of anticipated agreements [52].

$$\text{po} = \sum_{I=1}^{C} pij$$

$$\text{Pe} = \sum_{I=1}^{C} \text{piTpTj} \quad (2)$$

In this formula, pij stands for the ith and jth cells of the contingency table, piT for the total of all cells in the ith row, pTj for the total of all cells in the jth column, and c for the total number of raster categories. The contingency table, a matrix that depicts the frequency distribution of variables, is employed in this study to illustrate the relationship between the ith and jth cells [52]. The interactions between each cell in a matrix are tabulated and computed. The outcome reveals how each cell's criteria agreed as a whole [13]. As shown in Table 5, the constant kappa coefficient is an excellent sign of general agreement between thematically grouped maps and reference data [47]. The kappa approach is a different multiple-variable method for determining map categorization accuracy. It's derived from the error matrix and utilized for classification with the help of data reference [48]. The 2015 LCLU maps' resolution served as the main images for accurate assessment.

Several simulations were run using various combinations of geographical variables elements to forecasting the LULC change map for 2015. The overall accuracy and maximum Kappa coefficients for the different spatial variables The Variations of DEM, ranging from the road and built-up, all had a Kappa value of 73.45, according to the analysis. Many studies judged the maximum Kappa value of 79.27 percent a reasonable accuracy. As a result, it was determined that these variables significantly impact forecasting the LULC map of this basin. The LULC maps for 2025 and 2030 were then predicted using the same spatial variable combinations as the 2005 and 2010 LULC maps [52].

For transition potential modeling and prediction, we applied the CA-ANN technique. It projected LULC for 2015 using LULC data from 2005-2010 and spatial factors, and we got a validation kappa value of 0.87. When we compared the real LULC of 2020 with the predicted data after obtaining the projected LULC, we found that the projected data had an overall accuracy of 75.30 percent and an overall kappa value of 0.38. The maps and statistics for 2015 and 2020 are shown in Tables 6–8.

Table 6: Validation for prediction of land changes to 2010.

Class	Prediction area for 2015 (%)	Accuracy	Kappa value	
High land	1.57%			
Mountains	28.55%			
Land area	4.76%			
Builtup	41.48%	75.30	ANN 0.87	Validation 0.38
Vegetation	13.00%			
Bare land	10.64%			
Total of area=	100%			

Table 7: Validation for prediction of land changes to 2015.

Class	Prediction area for 2015 (%)	Accuracy	Kappa value	
High land	0.97%			
Mountains	10.72%			
Land area	15.63%			
Builtup	48.12%	79.10	ANN 0.77	Validation 0.49
Vegetation	20.95%			
Bare land	3.61%			
Total of area=	100%			

Table 8: Validation for prediction of land changes to 2020.

Class	Prediction area for 2020 (%)	Accuracy	Kappa value	
High land	3.30%			
Mountains	12.99%			
Land area	4.96%			
Builtup	49.28%	69.10	ANN 0.78	Validation 0.39
Vegetation	17.12%			
Bare land	2.36%			
Total of area=	100%			

Table 9: The Difference in land changes actual and prediction for the 2010 year.

Class	Actual area for 2010 (%)	Prediction area for 2010 (%)	The difference in land changes actual & prediction for 2010
High land	1.83%	1.57%	0.26%
Mountains	29.61%	28.55%	1.06%
Land area	5.53%	4.76%	0.77%
Builtup	40.15%	41.48%	-1.33%
Vegetation	12.85%	13.00%	-0.15%
Bare land	10.03%	10.64%	-0.61%
Total of area=	100%	100%	

Table 10: The Difference in land changes actual and prediction for the 2015 year.

Class	Actual area for 2015(%)	Prediction area for 2015 (%)	The difference in land changes actual & predicted for 2015
High land	2.41%	0.97%	1.44%
Mountains	36.75%	10.72%	26.03%
Land area	8.51%	15.63%	-7.12%
Builtup	30.94%	48.12%	-17.18%
Vegetation	16.31%	20.95%	-4.64%
Bare land	5.08%	3.61%	1.47%
Total of area=	100%	100%	

Table 11: The Difference in land changes actual and prediction for the 2020 year.

Class	Actual area for 2020 (%)	Prediction area for 2020 (%)	The difference in land changes actual & prediction for 2020
High land	3.30%	3.30%	-1.47%
Mountains	12.99%	12.99%	6.62%
Land area	4.96%	4.96%	0.57%
Builtup	49.28%	49.28%	-9.13%
Vegetation	27.12%	17.12%	-4.27%
Bare land	2.36%	2.36%	7.67%
Total of area=	100%	100%	

Table 12: Analysis of Land changes for years 2025,and 2030.

No	Class	Predicted 2025		Predicted 2030	
		AREA km^2	%	AREA km^2	%
1	High land	316881	1.83%	492039	2.41%
2	Mountains	5127039	29.61%	7512750	36.75%
3	Land area	957069	5.53%	1740402	8.51%
4	Builtup area	6952491	40.15%	6325785	55.94%
5	Vegetation	2224908	12.85%	3333969	16.31%
6	Bare land	1735965	10.03%	1037925	5.08%
7	Total of area=	1731435	100%	20442870	100%

The process of verifying the accuracy and reliability of the tool (MOLUSCE) for predicting land changes, which has been widely used in the recent period, and identifying the difference between actual and predicted changes in the land are unique ideas distinguished in this field. They are significant ideas compared to other studies.

3.2.7. Results. The results in Table 9 showed the accuracy and reliability of MOLUSCE for predicting land changes due to the difference between the actual. They predicted land changes for 2010 before the conflict in the region being very low. Where the percentage of Difference changes in land changes for actual and prediction (2010) are built-up area with -1.33%, bare land -0.61%, vegetation with -0.15%, high ground with 0.26%, the land area with -0.77%, and mountains with 1.06%, as described in Table 9.

The difference between land changes for actual and prediction changes (2015) described in Table 10 is clear where were built-up area with -17.18%, bare land with 1.47%, vegetation with -4.64%, high ground with 1.44%, a land area with -7.12%, and mountains with 26.03%. That indicates differences between actual and prediction changes due to events conflicting suddenly.

The difference in land changes for actual and prediction (2020) described in Table 11 are impacted by events in 2015. Built-up area is -9.13%, bare land with 7.67%, vegetation with -4.27%, high ground with -1.47%, a land area with 0.57%, and mountains with 6.62%, as.

The percentage of Difference land changes described in Table 13 for actual and prediction (2025 and 2030) are impacted by events in 2015. See Table 12.

A comparison of findings of the study revealed that 2015 was a dividing line in the changes that occurred in Sana'a, which showed that before 2015, the capital was in better shape. Sana'a was progressing in urban area density, with an increased built-up area. After 2015 the built-up area decreased. That means the region was affected negatively. The results also indicated the accuracy and reliability of MOLUSCE for predicting land changes. There has been an increase in the proportion of built-up and agricultural land. For the periods, there was no change in the area for the plantation and grassland classes. It has been highlighted that the amount of built-up and cropland may increase. Changes in land usage are also calculated as a proportion of the total land area. A positive value indicates an improvement in the rating, whereas a negative value shows a decrease in the rating. There was an increase in developed and agricultural land by 2030. A decline in volume is projected for other categories, excluding farms and grasslands. You can see from the analysis that when one classification's space grows, so does the area of the other classes, and vice versa.

The summary of the findings of this study is four points 1. The actual changes (2015) do not support the logical increasing tendency toward the advancement of the urban space since it is typical for the human element to advance to the increasing

construction every day, and the outcomes of land changes will be adverse. 2/prediction changes for (2010 and 2020) are consistent with the logical upward trend toward urban space progress. 3/The attempt to follow a logical, incremental trend towards improving urban space is supported by prediction changes for 2025–2030. 4/The results of land change actual and predicted for the 2010 map before conflicts were minimal, which proves MOLUSCE results accuracy and dependability in anticipating land changes are very high.

4. Discussion

Many articles have been received in recent years on land use analysis using the MOLUSCE tool, and each has different, essential, and profound results. To clarify the difference, we will put a focused comparison between this study and some studies received in recent years:

Manikandan Kamaraj and colleagues [51], with the MOLUSCE tool and the MLP-ANN model, could forecast and identify future land-use changes for 2025 and 2030 in the Bhavani basin for the two time periods, 2005 and 2015. While Muhammad et al. [4] conducted a study that resulted to: physical and financial driving factors have a considerable impact on landscape designs. Within the final three decades the forecasts (2030–2050) back the expanding drift towards an impenetrable surface at the cost of necessary amounts of woodland and green space. By Modeling, Rizwan Muhammad and colleagues [4] used the tool MOLUSCE to analyze the strength and evolution of spatiotemporal LULC trends during the preceding four decades. They were speculating on the future of LULC in light of social and environmental variables and calculating the magnitude of the LULC shift and any potential effects on the regional pattern. Setting up the circumstances for a future LULC intensity [53].

In the current study in 2010, the differences were tiny, very, very low, which means that changes were expected. But in 2015, the differences were more than 10%, which means that the changes were not expected. Also, in 2020 it was very little, less than 10%, which means that changes were expected. Thus the analysis of the results demonstrated the merit and superiority of the MOLUSCE model used to predict the results presented accurately, and the analysis details in the results section. The results revealed that after 2010, the built-up area on the 2010 map decreased while the land area increased. I was referring to the bad situation of Sana'a resulting from the conflict, with the increase in the building area in the city, which led to a decrease in land area & reduction in the building area in the growing land area in the city. The current study demonstrated that the conflict had caused LULC changes in the area mentioned in 2015. The MOLUSCE is coefficient reliability and accuracy for the forecast of land changes through comparison of this study between actual and predictive images of land changes before conflict (2010) map and after the conflict (2015) map, and which impacts on land changes in 2020,2025, and 2030.

In general, it's difficult to determine the difference between actual and predicted land changes without this research. The motivation behind this research was to pinpoint the differences where guessing them was difficult because land use is influenced by physical, economic, and human factors.

This research will assist in monitoring and predicting future land use and cover changes. Policymakers and decision-makers can use the study's findings to address the exploitation of natural resources in dry areas.

5. Conclusion

The study concluded that human factors and processes have greatly affected the shapes of the earth's surface. A comparison of findings of the study revealed that 2015 was a dividing line in the changes that occurred in Sana'a, which showed that before 2015, the capital was in better shape. Sana'a was progressing in urban area density, with an increased built-up area. In 2015 the built-up area decreased, and the region was affected negatively. Comparing actual and predicted land changes is critically important because it helps determine two cases. This study has dealt with these two cases for this comparison: In the case that the situation is stable in the area studied (2010), this comparison helps determine the feasibility and accuracy of the instrument used to predict Earth changes. In case the region is subjected to sudden and unexpected events such as conflict with missiles and attacks on land destruction (2015), a comparison has an influential role in measuring the extent of changes in the land.

All area parameters were shown of actual changes: highland, mountains, land area, built-up area, and vegetation. The study found that the built-up area was 12.17 percent in 2005 but jumped to 40.15% in 2010. It is typical, and the expansion will continue due to human activity in front of rising structures and urban development, without sudden events. But the built-up area decreased to 30.94%percent in 2015, then 49.28% in 2020. The remaining analysis parameters affected the results of the increase and decrease in land changes in the future 2025 and 2030.

The Recommendations from this study suggest paying attention to and supporting such studies that focus on developing nations because they have a good impact on their development and improvement of conditions and because they are sorely in need of them. This study also advises researchers to finish evaluating the tools used to predict the earth's changes by comparing and measuring the differences between the actual changes to the land and the expected changes and then comparing those tools to extract the one that differs the least from them. In this way, we can determine which tools are the most effective at predicting changes to the earth. This study also urges further investigations into forecasting land changes due to its numerous advantages of improving a country's conditions and creating effective strategic plans for its advancement.

Data Availability

(1) The nature of the data, images of satellite landsat8, has been downloaded from UGSG and output images after classification using RF classifier with software SAGA-QGIS and remote sensing techniques and GIS. (2) The data can be accessed in the (Google Drive) repository https://drive.google.com/drive/u/0/my-drive. (3) There are not any restrictions on data access.

Conflicts of Interest

The author(s) declare(s) that they have no conflicts of interest.

Funding

This research received no specific grant from any funding agency in the public, commercial, or not-for-profit sectors. I do not have any financial funding to support my manuscripts.

References

[1] N. R. Khwarahm, P. M. Najmaddin, K. Ararat, and S. Qader, "Past and future prediction of land cover land use change based on earth observation data by the CA–Markov model: a case study from Duhok governorate, Iraq," *Arabian Journal of Geosciences*, vol. 14, no. 15, pp. 1–14, 2021.

[2] S. Tadese, T. Soromessa, and T. Bekele, "Analysis of the current and future prediction of land use/land cover change using remote sensing and the CA-Markov model in Majang forest biosphere reserves of Gambella, southwestern Ethiopia," *The Scientific World Journal*, vol. 2021, Article ID 6685045, 18 pages, 2021.

[3] A. Khan and M. Sudheer, "Machine learning-based monitoring and modeling for spatio-temporal urban growth of Islamabad," *The Egyptian Journal of Remote Sensing and Space Science*, vol. 25, no. 2, pp. 541–550, 2022.

[4] R. Muhammad, W. Zhang, Z. Abbas, F. Guo, and L. Gwiazdzinski, "Spatiotemporal change analysis and prediction of future land use and land cover changes using QGIS MOLUSCE plugin and remote sensing big data: a case study of Linyi, China," *Land*, vol. 11, no. 3, p. 419, 2022.

[5] A. M. Y. Hakim, S. Baja, D. A. Rampisela et al., "Spatiotemporal change analysis and prediction of future land use and land cover changes using QGIS MOLUSCE plugin and remote sensing big data: a case study of Linyi, China," *Land*, vol. 11, no. 3, p. 419, 2022.

[6] S. Arif, "Spatial dynamic prediction of land-use/landcover change (case study: tamalanrea sub-district, Makassar city)," *IOP Conference Series: Earth and Environmental Science*, vol. 280, no. 1, article 012023, 2019.

[7] E. A. Alshari and B. W. Gawali, "Analysis of Machine Learning Techniques for Sentinel-2A Satellite Images," *Journal of Electrical and Computer Engineering*, vol. 2022, Article ID 9092299, 16 pages, 2022.

[8] H. A. Khawaldah, I. Farhan, and N. M. Alzboun, "Simulation and prediction of land use and land cover change using GIS, remote sensing and CA-Markov model," *Global Journal of Environmental Science and Management*, vol. 6, no. 2, pp. 215–232, 2020.

[9] R. Hamad, H. Balzter, and K. Kolo, "Predicting land use/land cover changes using a CA-Markov model under two different scenarios," *Sustainability*, vol. 10, no. 10, p. 3421, 2018.

[10] S. Das and R. Sarkar, "Predicting the land use and land cover change using Markov model: a catchment level analysis of the Bhagirathi-Hugli River," *Spatial Information Research*, vol. 27, no. 4, pp. 439–452, 2019.

[11] A. M. Hashim, A. Elkelish, H. A. Alhaithloul, S. M. El-Hadidy, and H. Farouk, "Environmental monitoring and prediction of land use and land cover spatio-temporal changes: a case study from El-Omayed biosphere Reserve, Egypt," *Environmental Science and Pollution Research*, vol. 27, no. 34, pp. 42881–42897, 2020.

[12] Y. Lu, P. Wu, X. Ma, and X. Li, "Detection and prediction of land use/land cover change using spatiotemporal data fusion and the cellular automata–Markov model," *Environmental Monitoring and Assessment*, vol. 191, no. 2, pp. 1–19, 2019.

[13] M. H. Saputra and H. S. Lee, "Prediction of land use and land cover changes for North Sumatra, Indonesia, using an artificial-neural-network-based cellular automaton," *Sustainability*, vol. 11, no. 11, p. 3024, 2019.

[14] S. W. Wang, L. Munkhnasan, and W. K. Lee, "Land use and land cover change detection and prediction in Bhutan's high altitude city of Thimphu, using cellular automata and Markov chain," *Environmental Challenges*, vol. 2, article 100017, 2021.

[15] D. Abijith and S. Saravanan, "Assessment of land use and land cover change detection and prediction using remote sensing and CA Markov in the northern coastal districts of Tamil Nadu, India," *Environmental Science and Pollution Research*, vol. 29, pp. 1–13, 2021.

[16] X. Chang, F. Zhang, K. Cong, and X. Liu, "Scenario simulation of land use and land cover change in mining area," *Scientific Reports*, vol. 11, no. 1, pp. 1–12, 2021.

[17] K. Kulkarni and P. A. Vijaya, "NDBI based prediction of land use land cover change," *Journal of the Indian Society of Remote Sensing*, vol. 49, no. 10, pp. 2523–2537, 2021.

[18] P. Kulithalai Shiyam Sundar and P. C. Deka, "Spatio-temporal classification and prediction of land use and land cover change for the Vembanad Lake system, Kerala: a machine learning approach," *Environmental Science and Pollution Research*, vol. 29, pp. 1–17, 2021.

[19] "Assessment of land use and disclosure of land change using remote sensing in the Tana Lake basin, northwest Ethiopia," *Environmental Science Cogent*, vol. 6, no. 1, article 1778998, 2020.

[20] E. A. Alshari and B. W. Gawali, "Development of classification system for LULC using remote sensing and GIS," *Global Transitions Proceedings*, vol. 2, no. 1, pp. 8–17, 2021.

[21] W. Fu, J. Ma, P. Chen, and F. Chen, "Remote sensing satellites for digital earth," in *Manual of Digital Earth*, Springer, Singapore, 2020.

[22] S. S. Rwanga and J. M. Ndambuki, "Accuracy assessment of land use/land cover classification using remote sensing and GIS," *International Journal of Geosciences*, vol. 8, no. 4, pp. 611–622, 2017.

[23] https://www.latlong.net/place/sana-a-yemen-10298.html.

[24] https://www.hrw.org/ar/world-report/2020/country-chapters/336718.

[25] https://www.hrw.org/world-report/2020/country-chapters/yemen#.

[26] E. A. Alshari and B. W. Gawali, "Evaluation of the potentials and challenges of land observation satellites," *Global Transitions Proceedings*, vol. 2, no. 1, pp. 73–79, 2021.

[27] D. Radočaj, J. Obhođaš, M. Jurišić, and M. Gašparović, "Global open data remote sensing satellite missions for land monitoring and conservation: a review," *Land*, vol. 9, no. 11, p. 402, 2020.

[28] A. Sarica, A. Cerasa, and A. Quattrone, "Random forest algorithm for the classification of neuroimaging data in Alzheimer's disease: a systematic review," *Frontiers in Aging Neuroscience*, vol. 9, p. 329, 2017.

[29] http://ww.programmersought.com/article/46743604859/.

[30] https://corporatefinanceinstitute.com/resources/knowledge/other/random-forest/.

[31] M. S. Navin and L. Agilandeeswari, "Multispectral and hyperspectral images based land use/land cover change prediction analysis: an extensive review," *Multimedia Tools and Applications*, vol. 79, no. 39-40, pp. 29751–29774, 2020.

[32] S. Paul, K. G. Saxena, H. Nagendra, and N. Lele, "Tracing land use and land cover change in peri-urban Delhi, India, over 1973–2017 period," *Environmental Monitoring and Assessment*, vol. 193, no. 2, pp. 1–12, 2021.

[33] S. Alqadhi, J. Mallick, A. Balha, A. Bindajam, C. K. Singh, and P. V. Hoa, "Spatial and decadal prediction of land use/land cover using multilayer perceptron-neural network (MLP-NN) algorithm for a semi-arid region of Asir," *Saudi Arabia. Earth Science Informatics*, vol. 14, pp. 1547–1562, 2021.

[34] R. Bala, R. Prasad, and V. P. Yadav, "Quantification of urban heat intensity with land use/land cover changes using Landsat satellite data over urban landscapes," *Theoretical and Applied Climatology*, vol. 145, no. 1-2, pp. 1–12, 2021.

[35] M. O. Sarif and R. D. Gupta, "Spatiotemporal mapping of Land Use/Land Cover dynamics using Remote Sensing and GIS approach: a case study of Prayagraj City, India (1988–2018)," *Environment, Development and Sustainability*, vol. 24, no. 1, pp. 888–920, 2021.

[36] M. Atasoy, "Assessing the impacts of land-use/land-cover change on the development of urban heat island effects," *Environment, Development and Sustainability*, vol. 22, no. 8, pp. 7547–7557, 2020.

[37] M. Rihan, M. W. Naikoo, M. A. Ali, T. M. Usmani, and A. Rahman, "Urban Heat Island dynamics in response to land-use/land-cover change in the Coastal City of Mumbai," *Journal of the Indian Society of Remote Sensing*, vol. 49, no. 9, pp. 2227–2247, 2021.

[38] R. K. Singh, V. S. P. Sinha, P. K. Joshi, and M. Kumar, "A multinomial logistic model-based land use and land cover classification for the south Asian Association for Regional Cooperation nations using moderate resolution imaging Spectroradiometer product," *Environment, Development and Sustainability*, vol. 23, no. 4, pp. 6106–6127, 2021.

[39] R. Ahmed, S. T. Ahmad, G. F. Wani, P. Ahmed, A. A. Mir, and A. Singh, "Analysis of landuse and landcover changes in Kashmir valley, India—a review," *GeoJournal*, vol. 85, pp. 1–13, 2021.

[40] S. Mansour, M. Alahmadi, P. M. Atkinson, and A. Dewan, "Forecasting of built-up land expansion in a desert urban environment," *Remote Sensing*, vol. 14, no. 9, p. 2037, 2022.

[41] X. Huang, L. Hao, G. Sun, Z. L. Yang, W. Li, and D. Chen, "Urbanization aggravates effects of global warming on local atmospheric drying," *Geophysical Research Letters*, vol. 49, no. 2, p. e2021GL095709, 2022.

[42] A. Masrur, A. Dewan, D. Botje, G. Kiselev, and M. M. Murshed, "Dynamics of human presence and flood-exposure risk in close proximity to Bangladesh's river network: an evaluation with multitemporal satellite imagery," *Geocarto International*, vol. 37, pp. 1–17, 2022.

[43] S. Abdullah, M. S. G. Adnan, D. Barua et al., "Urban green and blue space changes: a spatiotemporal evaluation of impacts on ecosystem service value in Bangladesh," *Ecological Informatics*, vol. 70, article 101730, 2022.

[44] E. Rottler, A. Bronstert, G. Bürger, and O. Rakovec, "Projected changes in Rhine River flood seasonality under global warming," *Hydrology and Earth System Sciences*, vol. 25, no. 5, pp. 2353–2371, 2021.

[45] H. Yohannes, T. Soromessa, M. Argaw, and A. Dewan, "Impact of landscape pattern changes on hydrological ecosystem services in the Beressa watershed of the Blue Nile Basin in Ethiopia," *Science of the Total Environment*, vol. 793, article 148559, 2021.

[46] H. Hayat, T. A. Akbar, A. A. Tahir, Q. K. Hassan, A. Dewan, and M. Irshad, "Simulating current and future river-flows in the Karakoram and Himalayan regions of Pakistan using snowmelt-runoff model and RCP scenarios," *Water*, vol. 11, no. 4, p. 761, 2019.

[47] M. A. Areeq and M. Aklan, *The Impacts of Land-Use Change on the Runoff Characteristics Using HEC-HMS Model: A Case Study in Wadi Al-Mulaikhy Sub-Watershed LQ 6DQD D EDVLQ*, EasyChair, Manchester, 2019.

[48] F. Al Nozaily, *Performance and Process Analysis of Duckweed-Covered Sewage Lagoons for High Strength Sewage-the Case of Sana'a, Yemen*, vol. 25, CRC Press, 2000.

[49] C. T. Sufian and M. Barra, "Energy investment and business climate report for observer countries. International Energy Chapter2016," 2016, https://yemenportal.unhabitat.org/wp-content/uploads/2020/11/01-Sanaa-City-Profile.pdf.

[50] https://www.coursehero.com/file/43207182/QuickHelppdf/.

[51] M. Kamaraj and S. Rangarajan, "Predicting the future land use and land cover changes for Bhavani basin, Tamil Nadu, India, using QGIS MOLUSCE plugin," *Environmental Science and Pollution Research*, vol. 29, pp. 1–12, 2022.

[52] M. Zhang, C. Zhang, A. A. Kafy, and S. Tan, "Simulating the relationship between land use/cover change and urban thermal environment using machine learning algorithms in Wuhan City, China," *Land*, vol. 11, no. 1, p. 14, 2022.

[53] Z. A. Rahaman, A. A. Kafy, A. A. Faisal et al., "Predicting microscale land use/land cover changes using cellular automata algorithm on the northwest coast of peninsular Malaysia," *Earth Systems and Environment*, pp. 1–19, 2022.

[54] A. A. Kafy, M. S. Rahman, M. M. Hasan, and M. Islam, "Modelling future land use land cover changes and their impacts on land surface temperatures in Rajshahi, Bangladesh," *Remote Sensing Applications: Society and Environment*, vol. 18, article 100314, 2020.